

## Electronic Supplementary Information

### **Atomic Fe hetero-layered coordination between g-C<sub>3</sub>N<sub>4</sub> and graphene nanomeshes enhances ORR electrocatalytic performance for zinc-air batteries**

*Congwei Wang<sup>a</sup>, Huifang Zhao<sup>a,b</sup>, Jie Wang<sup>a,b</sup>, Zheng Zhao<sup>a,b</sup>, Miao Cheng<sup>a,b</sup>, Xiaoyong Duan<sup>a</sup>, Qin Zhang<sup>a</sup>, Junying Wang<sup>a</sup> and Junzhong Wang<sup>a,b,\*</sup>*

<sup>a</sup>. CAS Key Laboratory of Carbon Materials, Institute of Coal Chemistry, Chinese Academy of Sciences, Taiyuan, 030001, P. R. China

<sup>b</sup>. Center of Materials Science and Optoelectronics Engineering, University of Chinese Academy of Sciences, Beijing 100049, P. R. China

\*Email: [wangjz@sxicc.ac.cn](mailto:wangjz@sxicc.ac.cn)

#### **Experimental Section**

##### **Chemicals.**

Graphite (99.95% purity) was obtained from Qingdao Huarun Graphite Co., Ltd., Chemically pure ferric chloride (FeCl<sub>3</sub>), hydrochloric acid (HCl, 37 %) and melamine were purchased from Sinopharm Chemical Reagent Co., Ltd. All aqueous solutions were prepared by deionized water. All chemicals were used without further purification.

##### **Synthesis of atomic iron embedded exfoliated g-C<sub>3</sub>N<sub>4</sub> (CN-Fe).**

Dicyandiamide (DCDA, 1 g) and ferric chloride were mixed at weight ratios (DCDA/FeCl<sub>3</sub>) of 1 %, 3 %, 5 % and 10 %, respectively, and the suspension was stirred for 60 min at 80 °C. The solution was then lyophilized, and the product was annealed in a covered crucible at a heating rate of 2.3 °C min<sup>-1</sup> to 550 °C for 2 h in Ar flow. After annealing, DCDA was converted to g-C<sub>3</sub>N<sub>4</sub> via a series of polymerizations while the iron atoms were coordinated in g-C<sub>3</sub>N<sub>4</sub> matrix. After cooling, the obtained yellowish powders were washed in hydrochloric acid (1 mol L<sup>-1</sup>) and deionized water to remove uncoordinated iron species. The as-made

porous bulk CN-Fe was then added into a mixture ( $v/v=1$ ) of deionized water and isopropanol (IPA) followed by probe sonication at 500 W for 10 h. The mixture was stationary for 24 h, and the supernatant was collected as exfoliated porous CN-Fe nanosheets. The CN-Fe samples with different Fe feeding ratios were denoted as CN-Fe-1, CN-Fe-3, CN-Fe-5 and CN-Fe-10, respectively. For comparison, the control sample of pure g-C<sub>3</sub>N<sub>4</sub> (CN) was also synthesized as listed above without the addition of ferric chloride.

### **Synthesis of atomic iron embedded mesh-on-mesh g-C<sub>3</sub>N<sub>4</sub> / nitrogen doped graphene nanomesh (NGM-CN-Fe) SAC.**

The electrochemically exfoliated graphene aqueous dispersion (5 mg ml<sup>-1</sup>) was mixed with dicyanamide and MgSO<sub>4</sub> solution with a mass ratio of graphene/dicyanamide /MgSO<sub>4</sub> of 1/5/1. After sonication for 2 hours and lyophilized, the mixture was then heated to 900 °C at a heating rate of 10 °C min<sup>-1</sup> under the argon atmosphere for 1 hour. The product was then washed with 10 % (volume ratio) HCl solution and water for several times sequentially, and dried overnight to make graphene nanomesh powder. [S1]. The obtained exfoliated porous CN-Fe nanosheets (0.2 g) and GM were dispersed in deionized water at a weight ratio of 1:1. DCDA (0.8 g) was then added as nitrogen source. The mixture was sonicated for 2 h, then hydrothermal at 120 °C for 12 h and dried into solid form followed annealing at 600 °C for 90 min to give the NGM-CN-Fe catalyst. CN-Fe was also mechanically mixed with Super-P (conductive additive), denoted as CN-Fe/SP, to evaluate the impact of conductive additive on the catalytic activity of CN-Fe.

### **Instrumental characterization.**

The scanning electron microscopy (SEM), transmission electron microscopy (TEM), X-ray diffraction (XRD) and X-ray photoelectron spectroscopy (XPS) were conducted as comprehensively listed in group's previous literature [S2]. HAADF-STEM was performed on a JEM ARM200F equipped with double aberration correctors in Institute of physics, Chinese Academy of Sciences, and a cold field emission gun operated at 200 kV. STEM images were recorded using a HAADF detector with a convergence angle of 25 mrad and a collection angle between 70 and 250 mrad. Under these conditions, the spatial resolution is ca. 0.08 nm. The <sup>57</sup>Fe Mössbauer spectra of the catalysts were acquired with a source of <sup>57</sup>Co in Rh. The Brunauer–Emmett–Teller (BET) specific surface area were deduced from the N<sub>2</sub> physical adsorption measurement data that were obtained using an ASAP 2010 Accelerated Surface Area and Porosimetry System. XANES measurements at Fe K-edge in transmission mode

were performed at the BL14W1 in Shanghai Synchrotron Radiation Facility. The electron beam energy was 3.5 GeV and the stored current was 230 mA (top-up). The raw data analysis was performed using IFEFFIT software package according to the standard data analysis procedures.

### **Electrochemical measurements.**

The electrochemical performances were investigated using a set of electrochemical methodologies, such as cyclic voltammetry (CV), rotating disk electrode (RDE) in a three-electrode electrochemical cell fitted with platinum wire as the counter electrode and Ag/AgCl as the reference electrode on an Autolab electrochemical analyser (PGSTAT204) and a MSR electrode rotator (PINE, US). The catalyst ink was prepared by mixing the catalyst (12 mg) with 3 ml ethanol-water (1:1) and 10  $\mu$ L Nafion with the assist of bath sonication. Subsequently, the catalyst was loaded on the surface of GC electrode surface (diameter: 5 mm) by drop casting and dried in air. It is noted that special care was taken to maintain the loading of the catalysts the same in all samples. All the experiments were conducted at room temperature, in an O<sub>2</sub> or N<sub>2</sub>-saturated 0.1 M KOH aqueous solutions as electrolyte. All samples were tested for 5 times for the consistence and commercial Pt-C catalyst (20 wt. %) was used for comparison. CV curves were measured at a scan rate of 50 mvs<sup>-1</sup> and LSV curves were at 10 mvs<sup>-1</sup> at the range of +0.2 to -0.8 V for ORR and 0.0 to 1.0 V for OER. Chronoamperometric curves were tested at -0.3 V in O<sub>2</sub> saturated 0.1 M KOH at a rotation speed of 1200 rpm. A custom-built zinc–air single battery with the zinc foil and the air electrode as the anode and the cathode, respectively, was fabricated. The air electrode was fabricated as follows: a certain amount of catalyst with 5 wt. % Nafion was sonicated and drop casted on carbon cloth, then dried at 60°C overnight. It is noted that the catalyst loading was kept at 0.5 mg cm<sup>-2</sup> for all batteries. The electrolyte was 6 M KOH aqueous solution with 0.2 M zinc acetate. Measurements were performed on the as-built battery cell at room temperature with a LAND multichannel battery testing system.

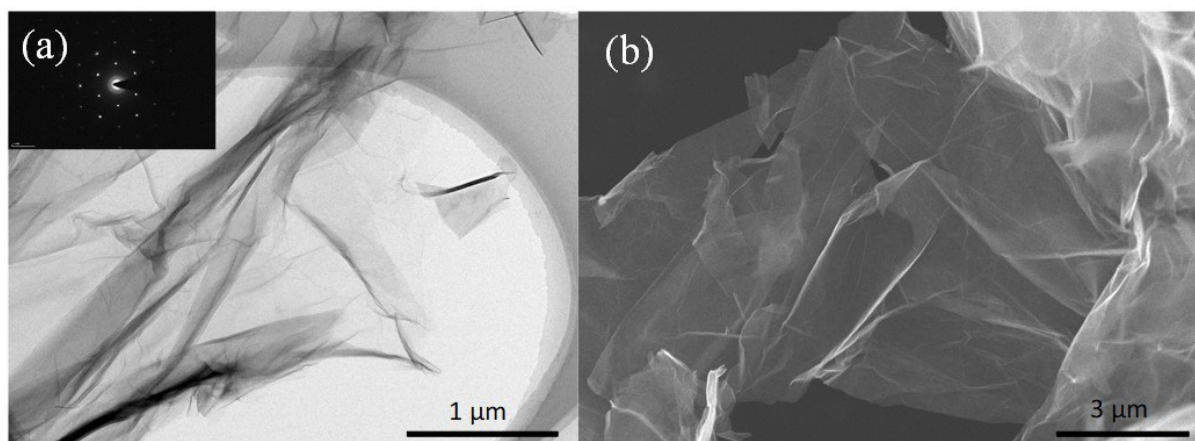


**Figure S1.** (a) TEM image of raw electrochemical exfoliated graphene sheets, the inset shows its SAED pattern, (b) SEM image of raw graphene sheet.

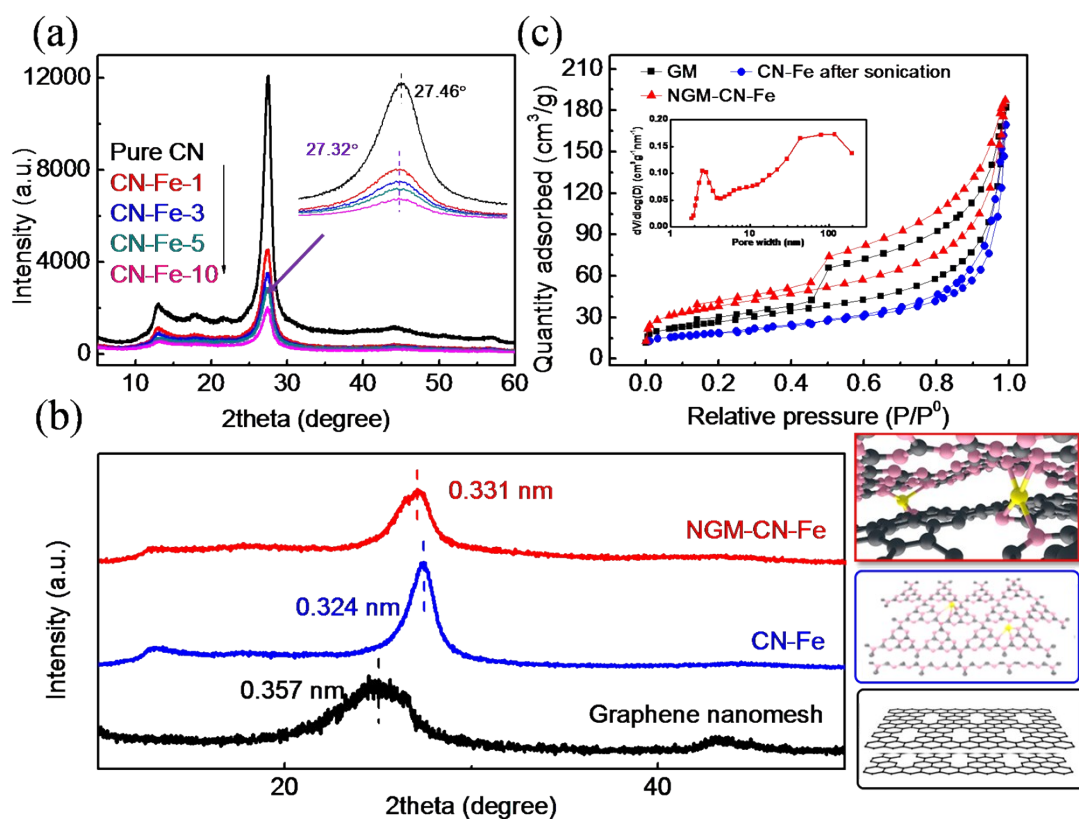


**Figure S2.** (a) XRD of pure CN and atomic Fe coordinated CN, (b) XRD of graphene nanomesh, CN-Fe and NGM-CN-Fe, the proposed inter-layer structure of samples are listed on side, (c) BET spectra of GM, CN-Fe and NGM-CN-Fe, inset shows the pore size distribution of NGM-CN-Fe.

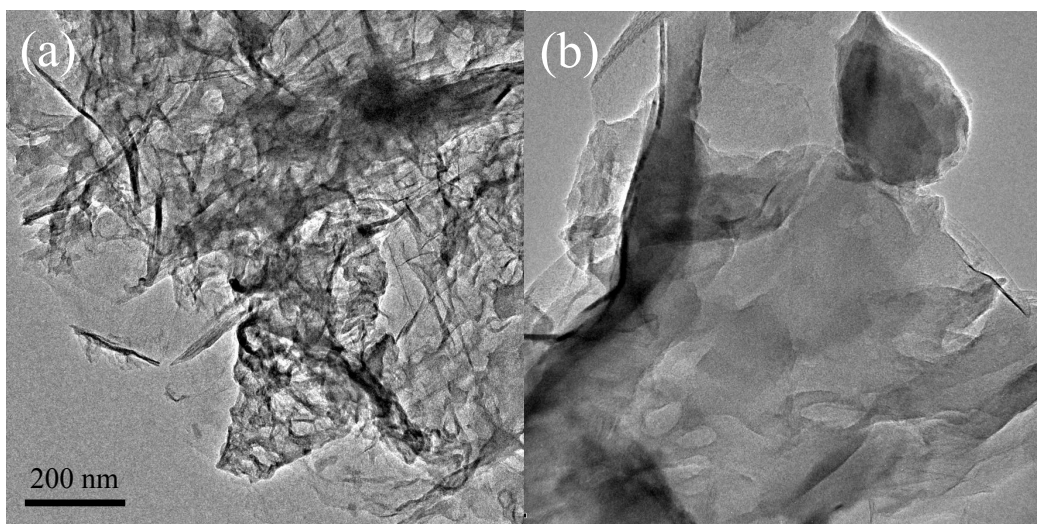


**Figure S3.** TEM image of obtained NGM-CN-Fe.

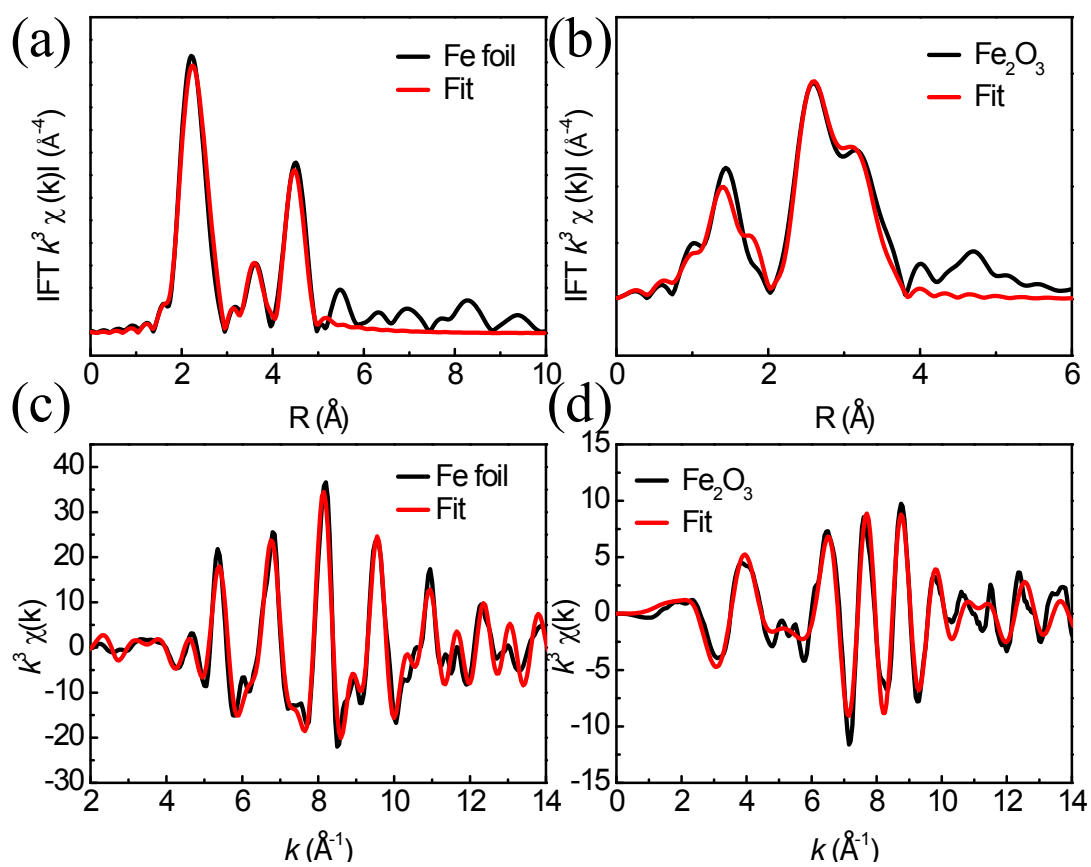


**Figure S4.** EXAFS spectra and fitting of (a) Fe foil and (b)  $\text{Fe}_2\text{O}_3$  and their corresponding fitting at  $k$  space (c-d).

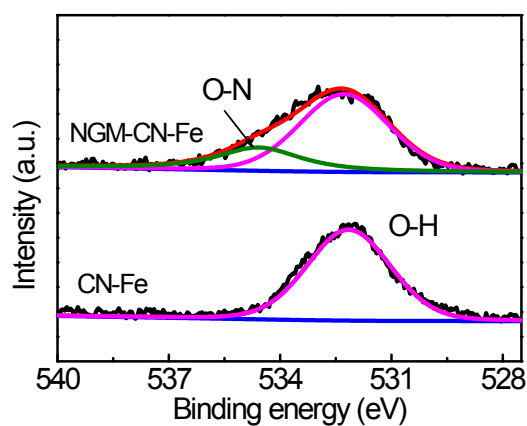


**Figure S5.** O 1s deconvolution XPS of CN-Fe and NGM-CN-Fe.

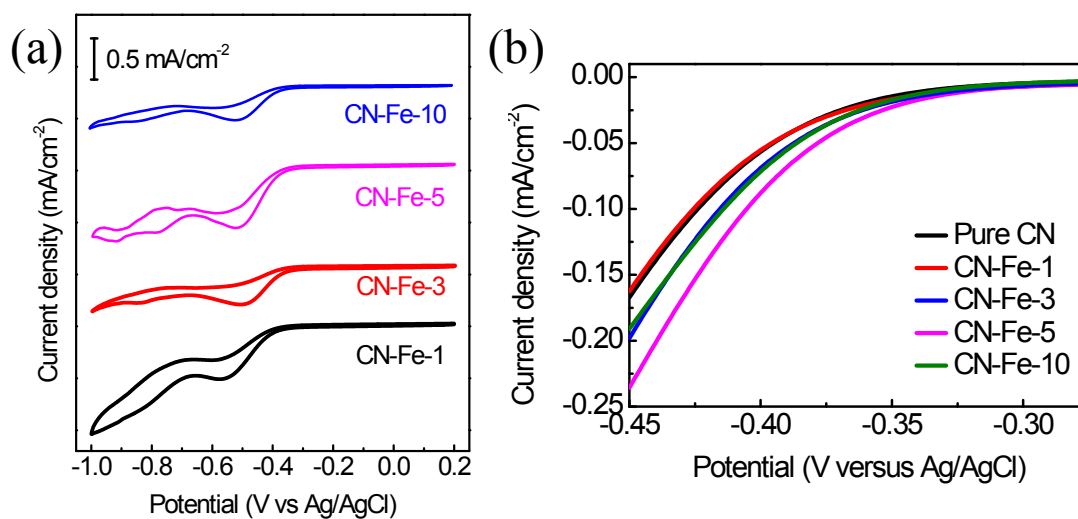


**Figure S6.** (a) CV curves of atomic Fe coordinated  $g\text{-C}_3\text{N}_4$  and their (b) LSV curves in electrolyte.

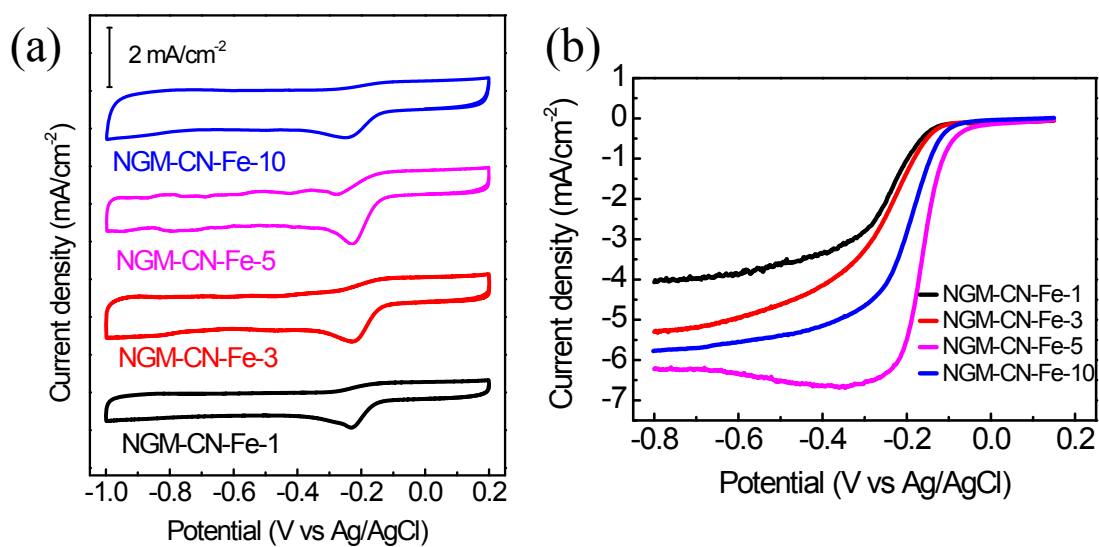


**Figure S7.** (a) CV curves of NGM-CN-Fe with different Fe feeding and their (b) LSV curves in electrolyte.

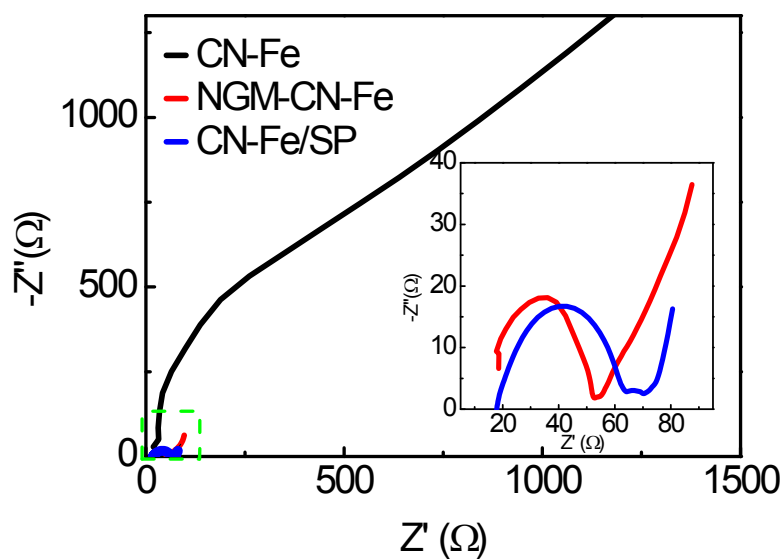


**Figure S8.** EIS Nyquist plots of CN-Fe, CN-Fe/SP and NGM-CN-Fe in a 0.1M KOH solution.

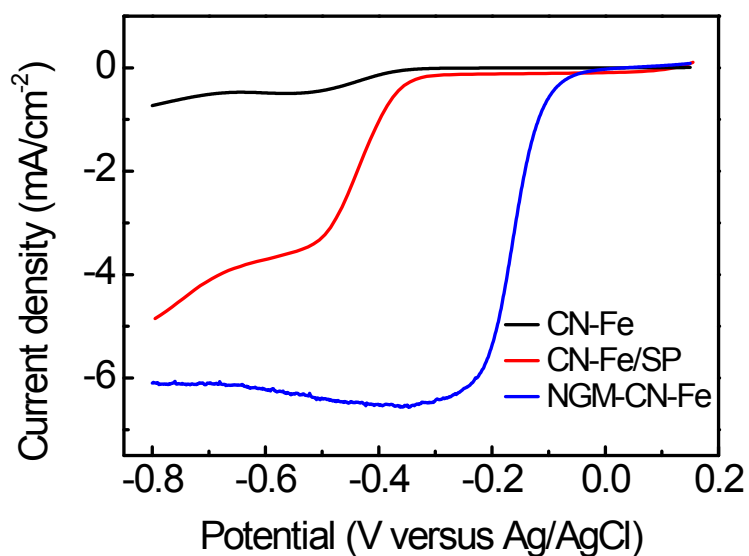


**Figure S9.** LSV curves of CN-Fe, NGM-CN-Fe and CN-Fe/SP.

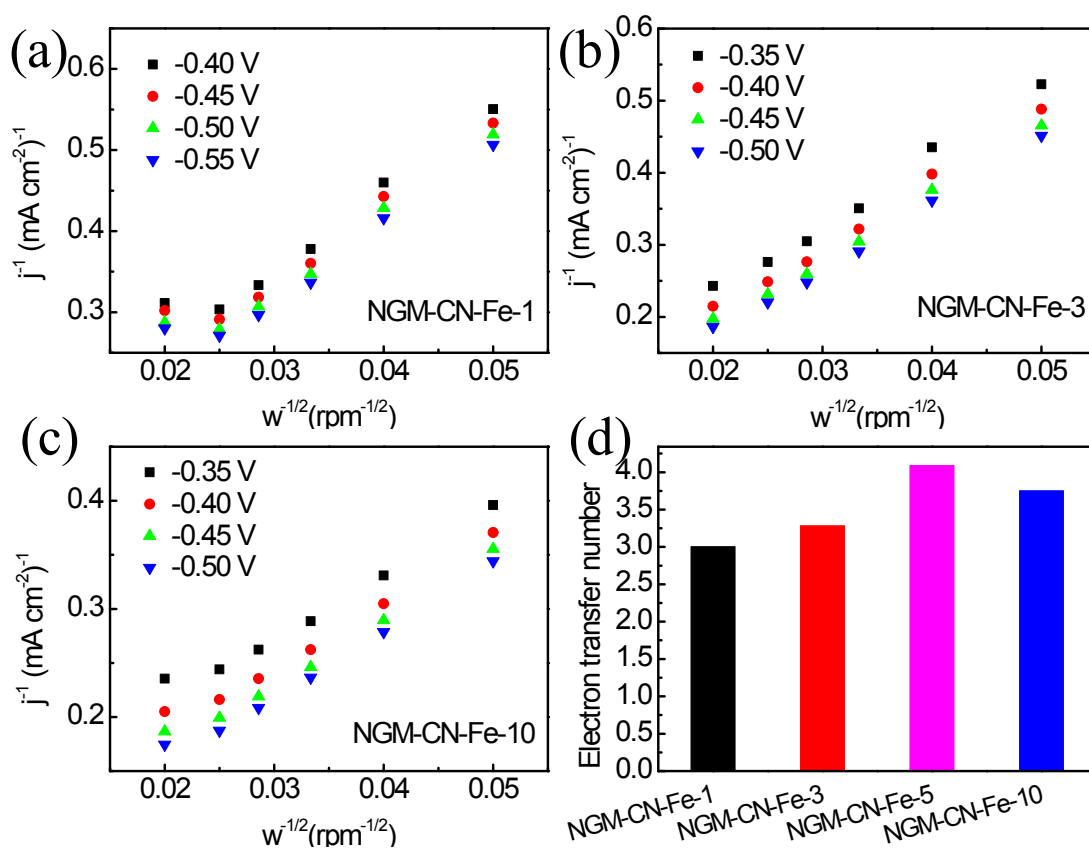


**Figure S10.** (a-c) K-L plot for NGM-CN-Fe-1, NGM-CN-Fe-3, NGM-CN-Fe-10, and (d) the calculated electron transfer number.

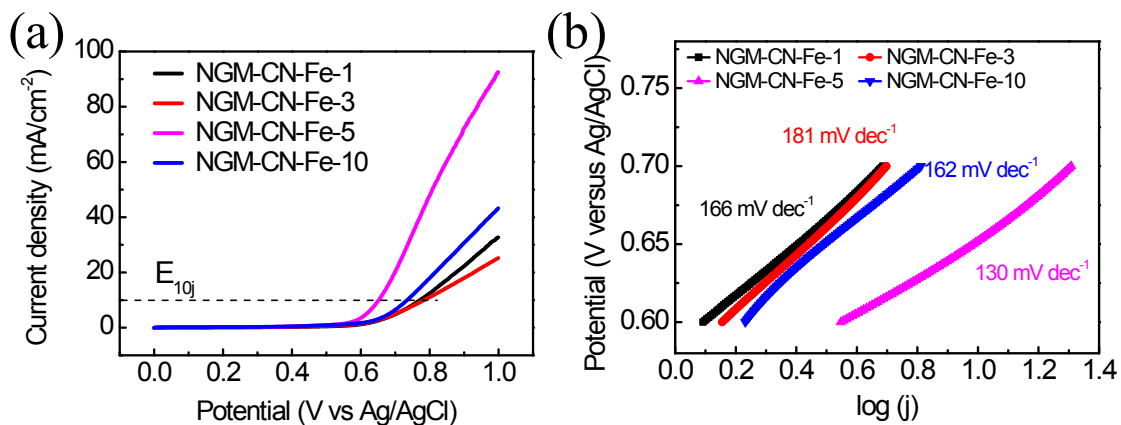


**Figure S11.** (a) LSV curve of NGM-CN-Fe-(1, 3, 5, 10) and their (b) Tafel plot.

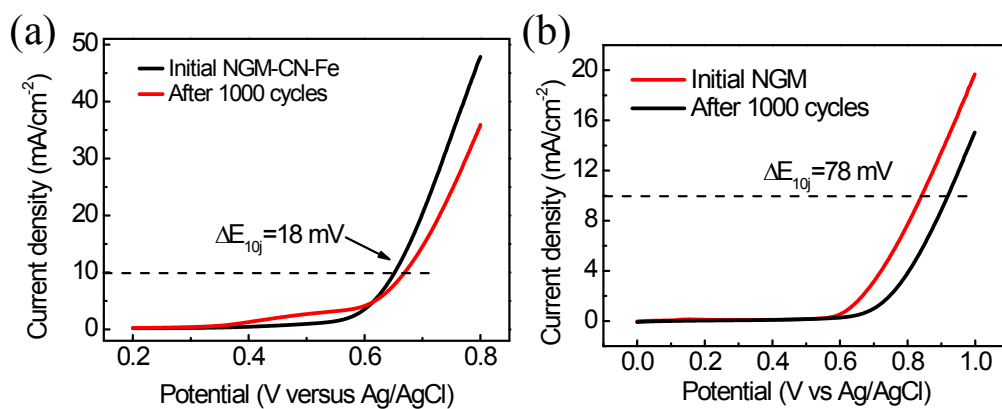


**Fig. S12** The comparison of NGM-CN-Fe and NGM durability via cyclic OER LSV measurement in 0.1 M KOH electrolyte.

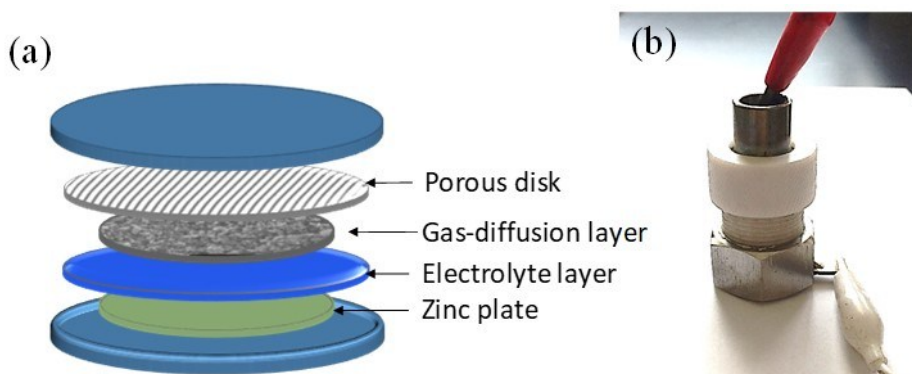


**Figure S13.** (a) Schematic graph and (b) optical photograph of custom-built ZAB cell. [S1]

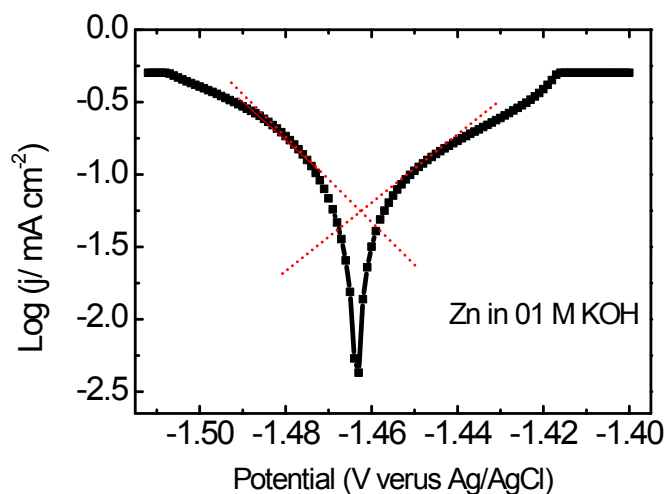


**Figure S14** Tafel plot of metallic Zn in 0.1 M KOH aqueous electrolyte.

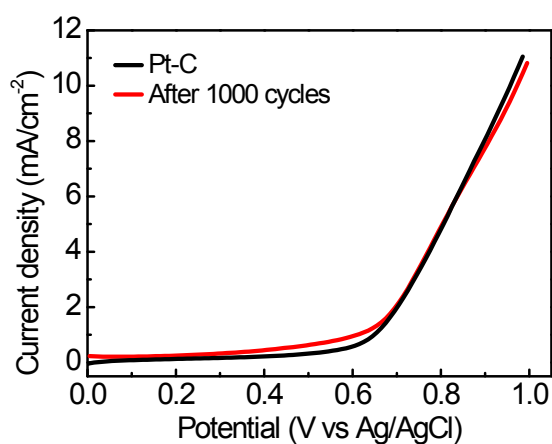


**Figure S15.** Durability test of Pt-C for OER in 0.1 M KOH electrolyte.

**Table S1.** Summary of detailed element contents in samples obtained by XPS.

Sample	C (at. %)	N (at. %)	Fe (at. %)	O (at. %)
CN	38.14	58.17	0.00	3.68
CN-Fe (-5)	39.31	53.94	1.38	5.37
NGM	93.25	3.42	0.00	3.33
NGM-CN-Fe (-5)	64.87	24.52	1.32	9.29

**Table S2.** Summary details of EFXAFS fitting parameters.

Sample	Path	N	R(Å)	$\sigma^2 (\times 10^{-3} \text{ \AA}^2)$	$\Delta E_0$ (eV)	R-factor
Fe foil	Fe-Fe1	8	2.48	6.4	7.03	0.008
	Fe-Fe2	6	2.85	5.3		
Fe <sub>2</sub> O <sub>3</sub>	Fe-O1	3	1.93	5.5	1.68	0.016
	Fe-O2	3	2.10	5.5		
FePc	Fe-N	3.89	2.05	4.3	6.78	0.027
<b>CN-Fe</b>	<b>Fe-N</b>	<b>3.61</b>	<b>2.09</b>	<b>8.6</b>	<b>0.79</b>	<b>0.007</b>
<b>NGM-CN-Fe</b>	<b>Fe-N</b>	<b>4.12</b>	<b>2.02</b>	<b>9.63</b>	<b>3.71</b>	<b>0.005</b>

**Table S3.** A comparison for a range of Fe based oxygen electrocatalysts and NGM-CN-Fe SAC.

Materials	Loading ( $\mu\text{g cm}^{-2}$ )	Onset potential (V vs. RHE)	Half-wave potential (V vs. RHE)	Ref
PCN-FeCo/C	200	1.00	0.85	S3
Fe-CNT-PA	500	0.93	0.80	S4
Fe-NMP, Fe-NMG	600	0.97	0.84	S5
COP@K10-Fe-900	200	0.97	0.85	S6
Fe-CB@PAN-1000	800	~0.98-1.00	0.88	S7
Fe <sub>3</sub> C/NG-800	400	1.03	0.86	S8
EDC4	600	0.96	0.80	S9
Fe-N-GC-900	600	1.01	0.86	S10
BIDC3	600	~1.00	~0.85	S11
Fe@BC-800	420	1.01	0.85	S12
Nb-in-C SAC complex	NA	0.834	~0.62	S13
Fe-NGM/C-Fe SAC	160	1.05	0.86	S2
Fe-ISAs/CN SAC	408	0.99	0.90	S14
Fe@C-FeNCs-2	700	~1.00	0.90	S15
Fe-Por-CNT SAC	NA	0.865	-	S16
MF-Fe-800 SAC	400	0.98	0.83	S17
PANI-Fe/Silica	100	0.84	0.73	S18
SA-Fe/NHPC SAC	100	-	0.87	S19
Fe <sub>SA</sub> -N-C SAC	280	-	0.89	S20
SA-Fe/NG SAC	240	0.90	0.80	S21
<b>NGM-CN-Fe</b>	<b>160</b>	<b>0.97</b>	<b>0.81</b>	<b>This work</b>

## References

- [S1] Wang, C.; Zhao, Z.; Li, X.; Yan, R.; Wang, J.; Li, A.; Duan, X.; Wang, J.; Liu, Y.; Wang, J. *ACS Appl. Mater. Interfaces*, **2015**, *9*, 41273.
- [S2] Wang, C.; Zhang, H.; Wang, J.; Zhao, Z.; Wang, J.; Zhang, Y.; Cheng, M.; Zhao, H.; Wang, J. *Chem. Mater.* **2017**, *29*, 9915.
- [S3] Lin, Q.; Bu, X.; Kong, A.; Mao, C.; Bu, F.; Feng, P. *Adv. Mater.* **2015**, *27*, 3431.
- [S4] Yang, G.; Choi, W.; Pu, X.; Yu, C. *Energy Environ. Sci.* **2015**, *8*, 1799.
- [S5] Hossen, M. M.; Artyushkova, K.; Atanassov, P.; Serov, A. *J. Power Sources* **2018**, *375*, 214.
- [S6] Guo, J.; Cheng, Y.; Xiang, Z. *ACS Sustainable Chem. Eng.* **2017**, *5*, 7871.
- [S7] Chen, J. L.; Li, W. B.; Xu, B. Q. *J. Colloid Interface Sci.* **2017**, *502*, 44.
- [S8] Xiao, M. L.; Zhu, J. B.; Feng, L. G.; Liu, C. P.; Xing, W. *Adv. Mater.* **2015**, *27*, 2521.

- [S9] Gokhale, R.; Chen, Y.; Serov, A.; Artyushkova, K.; Atanassov, P. *Electrochem. Commun.* **2016**, *72*, 140.
- [S10] Kong, A.; Zhu, X.; Han, Z.; Yu, Y.; Zhang, Y.; Dong, B.; Shan, Y. *ACS Catal.* **2014**, *4*, 1793.
- [S11] Gokhale, R.; Chen, Y.; Serov, A.; Artyushkova, K.; Atanassov, P. *Electrochim. Acta* **2017**, *224*, 49.
- [S12] Ma, X.; Lei, Z.; Feng, W.; Ye, Y.; Feng, C. *Carbon* **2017**, *123*, 481.
- [S13] Zhang, X.; Guo, J.; Guan, P.; Liu, C.; Huang, H.; Xue, F.; Dong, X.; Pennycook, S. J.; Chisholm, M. F. *Nat. Commun.* **2013**, *4*, 1924.
- [S14] Jiang, W. J.; Gu, L.; Li, L.; Zhang, Y.; Zhang, X.; Zhang, L. J.; Wan, L. J. *J. Am. Chem. Soc.* **2016**, *138*, 3570.
- [S15] Chen, Y.; Ji, S.; Wang, Y.; Dong, J.; Chen, W.; Li, Z.; Li, Y. *Angew. Chem. Int. Ed.* **2017**, *56*, 6937.
- [S16] Lee, D. H.; Lee, W. J.; Lee, W. J.; Kim, S. O.; Kim, Y. H. *Phys. Rev. Lett.*, **2011**, *106*, 175502.
- [S17] Lu, B.; Smart, T. J.; Qin, D.; Lu, J. E.; Wang, N.; Chen, L.; Peng, Y.; Ping, Y.; Chen, S. *Chem. Mater.* **2017**, *29*, 5617.
- [S18] Liang, H. W.; Wei, W.; Wu, Z. S.; Feng, X.; Müllen, K. *J. Am. Chem. Soc.* **2013**, *135*, 16002.
- [S19] Zhang, Z.; Gao, X.; Dou, M.; Ji, J.; Wang, F. *Small*, **2017**, *13*, 1604290.
- [S20] Jiao, L.; Wan, G.; Zhang, R.; Zhou, H.; Yu, S. H.; Jiang, H. L. *Angewandte Chemie*, **2018**, *130*, 8661-8665.
- [S21] Yang, L.; Cheng, D.; Xu, H.; Zeng, X.; Wan, X.; Shui, J.; Xiang, Z.; Cao, D. *Proc. Natl. Acad. Sci. U.S.A.*, **2018**, 201800771.